DENSIFICATION AND DEFORMATION DURING UNIAXIAL COLD COMPACTION OF STAINLESS STEEL POWDER WITH DIFFERENT PARTICLE SIZE

I. Cristofolini[a, *], G. Pederzini[b, 1], A. Rambelli[b, 2], A. Molinari[a, 3]

[a] Department of Industrial Engineering - DII, Via Sommarive 9, 38123, Trento, Italy
[b] Technical Department (Special Pressing) - Sacmi Imola S.C., Via Provinciale Selice 17/a – 40026 Imola (BO) - Italy

[*] Corresponding author. Phone: +39 0461 282509, Fax: +39 0461 282599, E-mail: ilaria.cristofolini@unitn.it

[1] Phone: +39 0542 607498, Fax: +39 0542 642354, E-mail: Gianluca.Pederzini@sacmi.it
[2] Phone: +39 0542 607111, Fax: +39 0542 642354, E-mail: Alex.Rambelli@sacmi.it
[3] Phone: +39 0461 282441, Fax: +39 0461 281977, E-mail: alberto.molinari@unitn.it

ABSTRACT
The behaviour of austenitic stainless steel powder column during uniaxial cold compaction was investigated in this work. Powders with different particle size were compacted to the same green density in a hydraulic press, also providing different H/D ratios in order to account for the influence of geometry. The analysis of the data continuously recorded by the press allowed distinguishing the contribution of the reversible phenomena (elastic deformation of powders and tools) and of the irreversible phenomena (rearrangement and plastic deformation of the powders). An analytical model for densification was proposed, considering both density and increase in density versus the applied pressure. The trend of reversible and permanent deformations versus the applied pressure was evaluated, also proposing an analytical model. The comparison between the densification curves and the curves of permanent deformation allowed highlighting the physical meaning of the model describing the increase in density for the different particle size.

Keywords: cold compaction, hydraulic press, powder behaviour in compaction.

1. INTRODUCTION
The properties and precision of final parts derive from powder behaviour during cold compaction, as it affects green density and density homogeneity and distribution [1], which are determined by the deformations induced by the compaction force. The compaction force is neither completely nor perfectly homogeneously conveyed to the powder column, due to the presence of frictional forces, both with the die walls and interparticle ones, and the resistance of the powder to elastic and plastic deformation depends on several variables. The powder behaviour during cold compaction, in fact, is affected by the composition and type of powder (prealloyed or blended), the size, morphology, and size distribution of particles, the homogeneity of particle packing after filling, the lubricant, the compaction strategy, the complexity of the geometry, and the continuously increasing density and extension of the interparticle contact areas.
The mechanics of cold compaction has been extensively studied, and several models have been proposed and compared with the experimental data. Most of the models derive from numerical simulations based on continuous mechanics, as by Cocks [2], Rossi et al. [3], Smith et al. [4].

Coube et al. considered the influence of die filling and powder transfer [5], also focusing on the problem of cracking during compaction [6], as previously Long [7]. Wall friction coefficient was considered in the simulation proposed by Wickmann et al.[8], while Ernst and Barnekow experimentally observed that friction coefficient with die walls decreases on increasing the applied pressure [9]. Al-Qureshi et al. proposed a model comprehending both a coefficient of friction with the die walls and an interparticle friction coefficient [10], also evaluating the effect of the morphology of powder particles [11]. The friction coefficient with punches was analysed by Bocchini, which highlighted its influence on the homogeneity in densification [12]. The influence of powder morphology was studied by Poquillon et al. [13], while Olsson and Larsson analysed the effect of particle size distribution [14]. R.M. German et al. [15] proposed a model for densification accounting for particle size up to nanoscale size range, which is based on the plasticity theory for porous bodies [16].

An alternative approach is focused on identifying the densification equation, defining a relationship between green density and compaction pressure. Several relationships were proposed in the literature by many authors. Most of them were reviewed in 1991 by Rong-de [17], who proposed a compaction equation based on a critical analysis of the models available at that time, and in 2002 by Secondi [18], who proposed a new equation, adequately representing the different models proposed by other authors with a proper identification of the considered parameters. Recently Aryanpour proposed a densification model based on the "piston equation" [19].

Nevertheless, the variety of the numerous parameters involved enhances the difficulty of obtaining a reliable model representing the powder behaviour during compaction, and also explains the differences in the models above.

This work is part of a large project aimed at experimentally obtaining an analytical model, which describes the powder behaviour during cold compaction by means of the data recorded by the press in terms of forces and displacements. In previous works the relationships between force and deformation during sizing have been successfully investigated using the same approach [20-22].

In this work, according to the procedure previously proposed [23, 24], the recorded data have been processed obtaining force versus displacement curves, and, in turn, permanent and reversible displacements, as affected by particle size, have been calculated. The behaviour of the powder is analysed with reference to the column of powder within the die, and to the maximum axial stress on the powder column. Work is in progress considering the multiaxial stress condition, and the gradients of both the axial and radial stresses along the compaction direction, as by the approach of the plasticity theory for porous bodies.

This analysis allowed describing the density and the increase in density during compaction, as affected by particle size. The contribution of the reversible and irreversible phenomena during the compaction cycle has been distinguished, and a model has been proposed to describe the relationships between deformations and applied stress in the different compaction conditions.

2. EXPERIMENTAL PROCEDURE

A commercial water atomised austenitic stainless powder - AISI 316L - was sieved in three particle size ranges: <45 μm, 45÷90 μm, 90÷125 μm. The tap density of the three powders was calculated from the filling height of the die cavity during the compaction experiments. Results are shown in Figure 1, where the tap density of the standard powder is also reported.

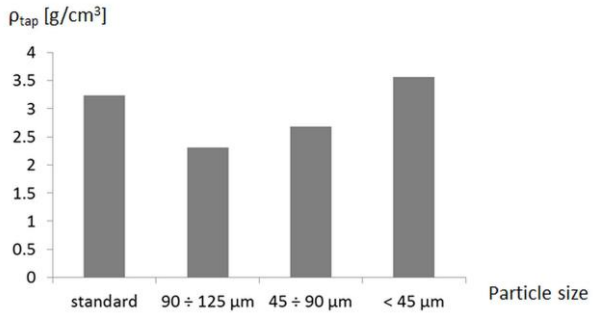

Figure 1. Tap density of the three powders studied and of the standard powder

Tap density significantly increases on decreasing the particle size.
The powders were compacted using a 200 tons hydraulic press, equipped with 9 hydraulic and 1 electric closed-loop controlled axes.
Cylindrical specimens were produced in a rigid die, 35.01 mm diameter, at 6.5 g/cm^3 green density, and two different H/D ratios (0.5, 1). The same amount of powder was also compacted at different levels of force, smaller than the maximum one, to collect data and obtain green parts corresponding to the different steps of the compaction process.
A "double action" pressing cycle was obtained moving down the die at half the speed of the upper punch. Different parameters were continuously recorded during compaction, the following have been considered in this study: F, compaction force, the force applied to the crosshead (related to the force applied to the powder column by the upper punch); X, the position of the lower surface of the upper punch with respect to the upper surface of the lower punch (as derived from the distance measured by two encoders fixed to the crosshead and to the base plate of the press, respectively); Z, the position of the upper surface of the die, again with respect to the upper surface of the lower punch (as derived from the distance measured by two encoders fixed to the die and to the base plate of the press, respectively). Figure 2 shows an example of the curves of both X and Z versus time, together with the curve of the compaction force (F), at the highest force applied (45÷90 µm, H/D 1). The steps of compaction, unloading and ejection are clearly identified.

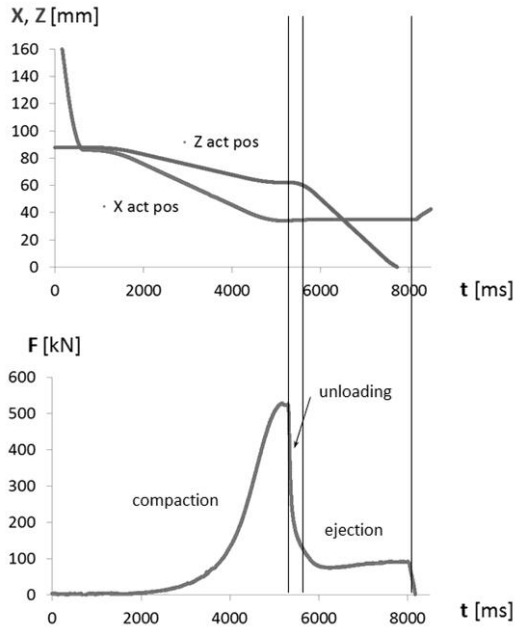

Figure 2. X, Z, and F versus time at the highest force - 45÷90 µm, H/D 1

To investigate the powder behaviour during compaction, the force/displacement compaction curves have been derived from the data recorded by the press. The starting point of the curve (zero displacement) corresponds to the X position measured when the punch contacts the powder and the die starts moving down (start of double action pressing). An example is shown in figure 3, where the reversible and permanent displacements are distinguished. Both the force and the displacement are reported as absolute values, being the force compressive and the recorded position continuously decreasing during compaction.

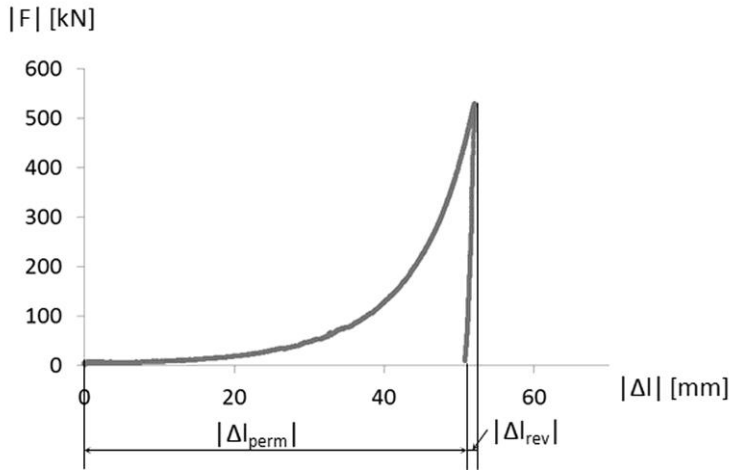

Figure 3. Example of force vs. displacement compaction curve - 45÷90 µm, H/D 1

The displacement is measured by two encoders, respectively on the crosshead and on the base plate, so it is also affected by the elastic deformation of the tools (punches, bearings and the plate supporting the die). Reversible displacements (related to elastic deformations of the tools and the powder column) and permanent displacements (related to rearrangement and plastic deformation of the powder column) contribute to the total displacement, as by equation (1)

$$\Delta l_{tot} = \Delta l_{rev} + \Delta l_{perm} = \Delta l_{el_{tools}} + \Delta l_{el_{powder}} + \Delta l_{rearr_{powder}} + \Delta l_{plast_{powder}} \quad (1)$$

3. RESULTS AND DISCUSSION

3.1 Densification curve

The densification curve correlates the density to the compaction pressure. Here the actual density (density of the powder column within the die) was calculated from the mass and the actual height of powder column during compaction. Such a height was obtained by the X position, to which the contribution due to the elastic contraction of the tools at each pressure was added. The difference between actual density and green density (as measured on the green parts after ejection) is 1% maximum, in all the considered conditions. Figure 4 shows the density versus the applied pressure, for each particle size, and H/D ratio.

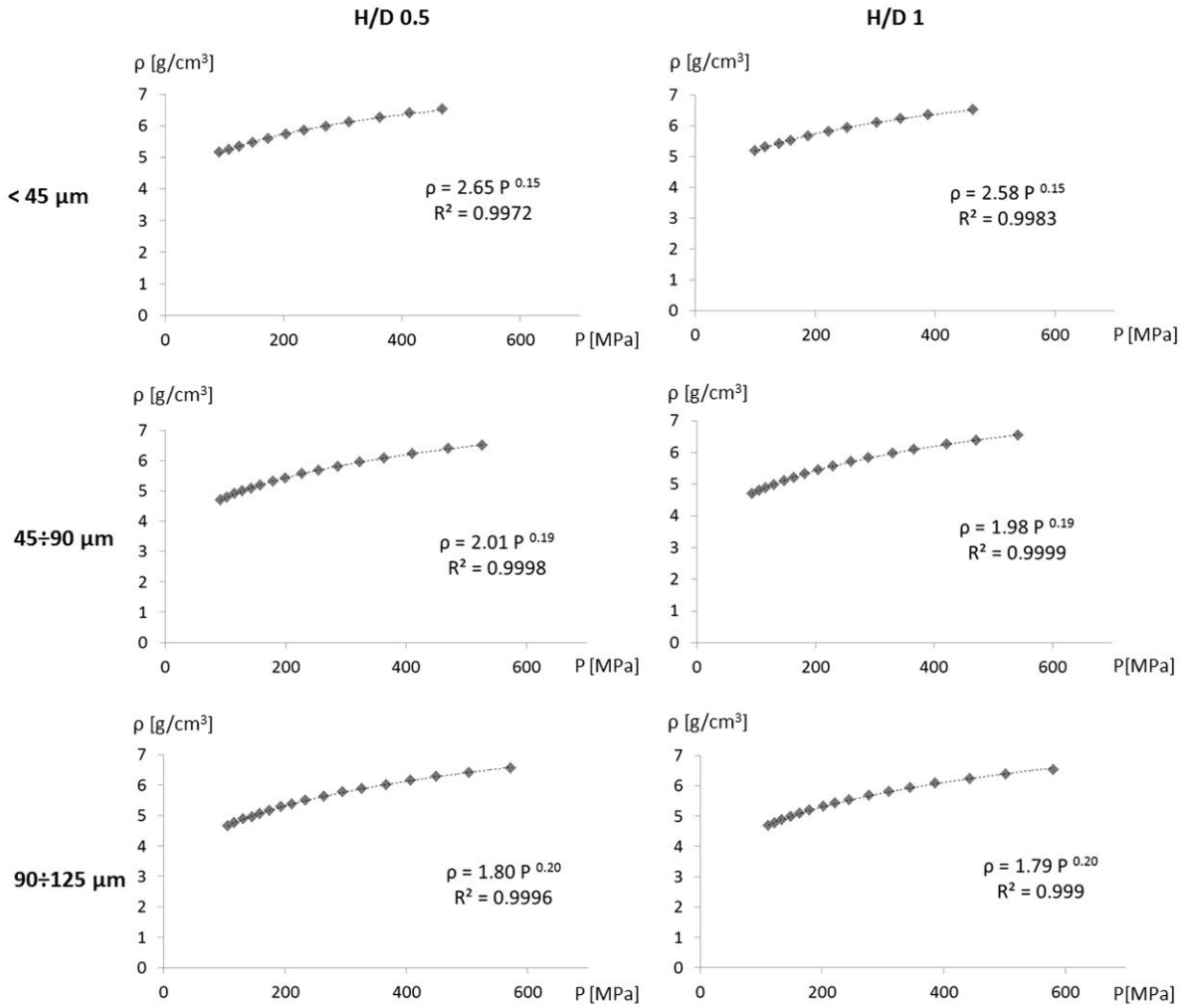

Figure 4. actual density vs. applied pressure for each particle size and H/D ratio

The exponential fit provides the model for densification accounting for the progressive increase in the resistance offered by the powder column, according to equation (2)

$$\rho = aP^b \tag{2}$$

Parameter *a* is a measure of the compressibility of the powder column, while *b* is a measure of the attitude of the material to increase its density on increasing pressure.
Figure 5 shows parameters *a* and *b*, as affected by both particle size and H/D ratio.

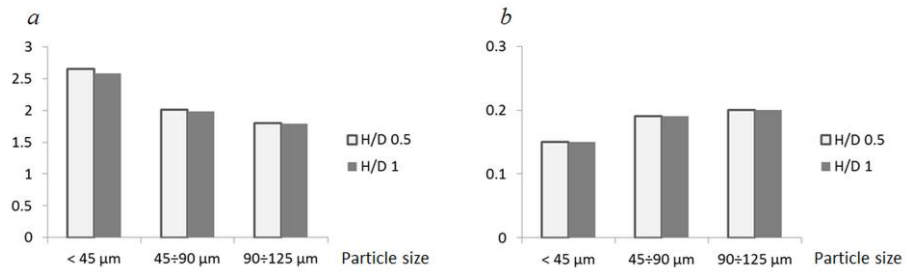

Figure 5. parameters *a* and *b*, as affected by both particle size and H/D ratio

No influence of H/D ratio is observed on both *a* and *b* parameters. This is likely due to the range of H/D ratios investigated, which does not allow highlighting a significant influence of frictional forces. Further work is in progress to investigate higher H/D ratios.
Increasing particle size, parameter *a* slightly decreases and *b* slightly increases correspondingly, meaning a lower compressibility, but a slightly higher attitude of the material to increase its density on increasing pressure. Nevertheless, these differences are mainly observed at the lower pressure, as it results from figure 6, where all the densification curves are plotted on the same graph, grouped by H/D ratio.

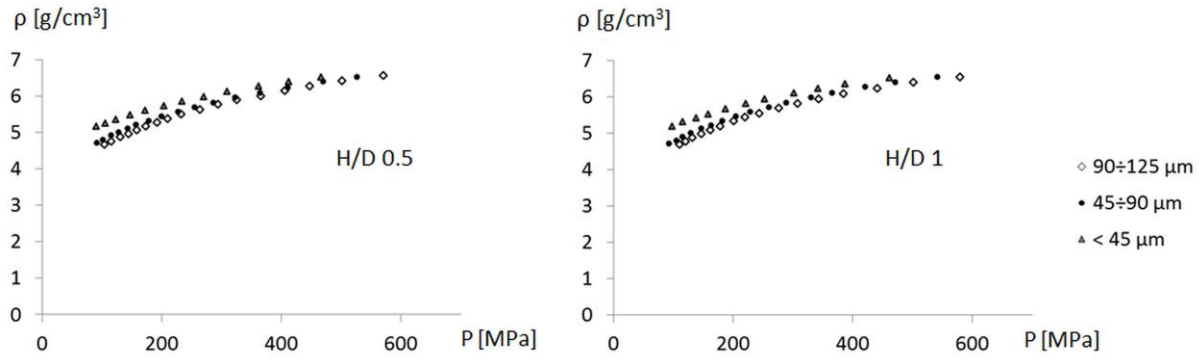

Figure 6. Actual density vs. applied pressure for each particle size grouped by H/D ratio

At the end of compaction all the curves tend to overlap, so that the main differences are attributable to the first compaction steps, where an important role is played by rearrangement, which is strongly influenced by the tap density. To highlight these differences, densification curves are expressed in terms of increase in density, considering the difference between actual density and tap density in equation (3)

$$\rho - \rho_{tap} = a' P^{b'} \tag{3}$$

Figure 7 compares the curves of the increase in density versus the applied pressure for the different particle sizes, grouped by H/D ratio.

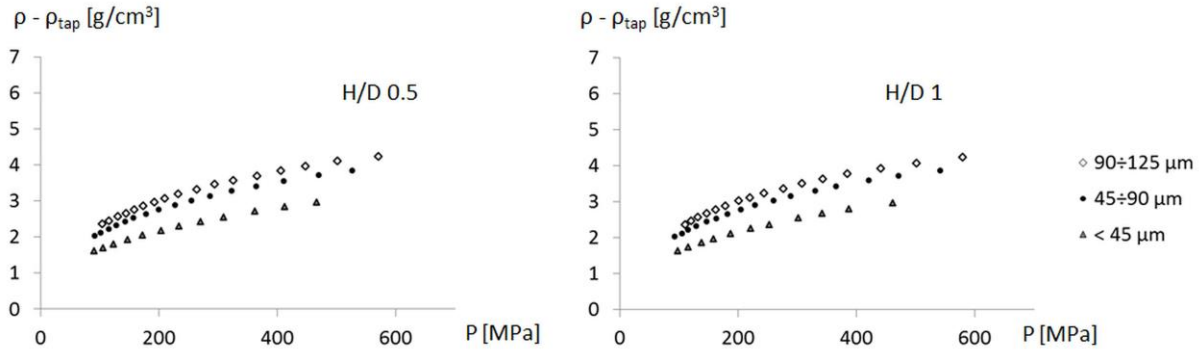

Figure 7. Increase in density vs. applied pressure for each particle size grouped by H/D ratio

The increase in density shown in figure 7 is the highest for the largest particle size, due to its lowest tap density. Figure 8 shows parameters *a'* and *b'*, as affected by both particle size and H/D ratio.

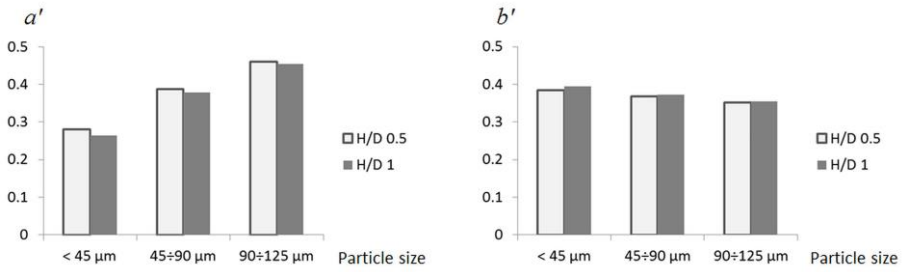

Figure 8. Parameters *a* and *b*, as affected by both particle size and H/D ratio

3.2 The force/displacement compaction curve

Figure 9 shows the force vs. displacement curves at the maximum force for each particle size, and H/D ratio.

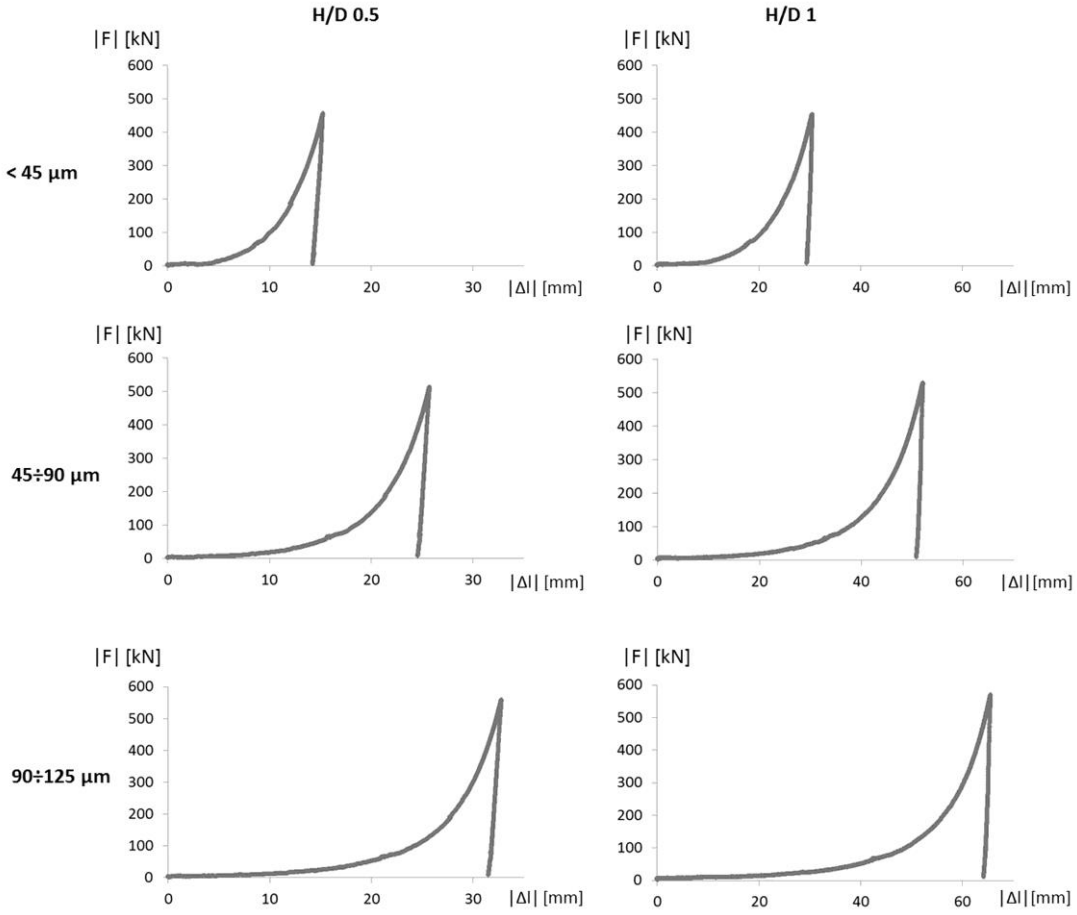

Figure 9. Force vs. displacement curves at the maximum force for each particle size and H/D ratio

Both the force and the total displacement increase with the particle size, whilst no significant effect of the H/D ratio is observed. The effect of particle size on the total displacement is due to the different tap density: the lower the tap density, the higher the displacement to obtain the same green height. Higher displacements also imply larger sliding of the powder particles against the die wall, which implies a higher dissipation of force due to friction. Interparticle friction, instead, can be related to the effect of particle size on the force. Interparticle friction

is expected to decrease on increasing particle size, thus determining an increase in the radial-to-axial force ratio, larger frictional forces against the die wall and, in turn, larger axial force gradients.
A detailed analysis of the forces acting on the powders during compaction as a function of the particle size is in progress.

3.3 Reversible and permanent displacements

Reversible displacement is attributable to the elastic displacement of the tools and the powder column, as by equation (4)

$$\Delta l_{rev} = \Delta l_{el_{tools}} + \Delta l_{el_{powder}} \tag{4}$$

Figure 10 shows the reversible displacement versus compaction force for each particle size and H/D ratio

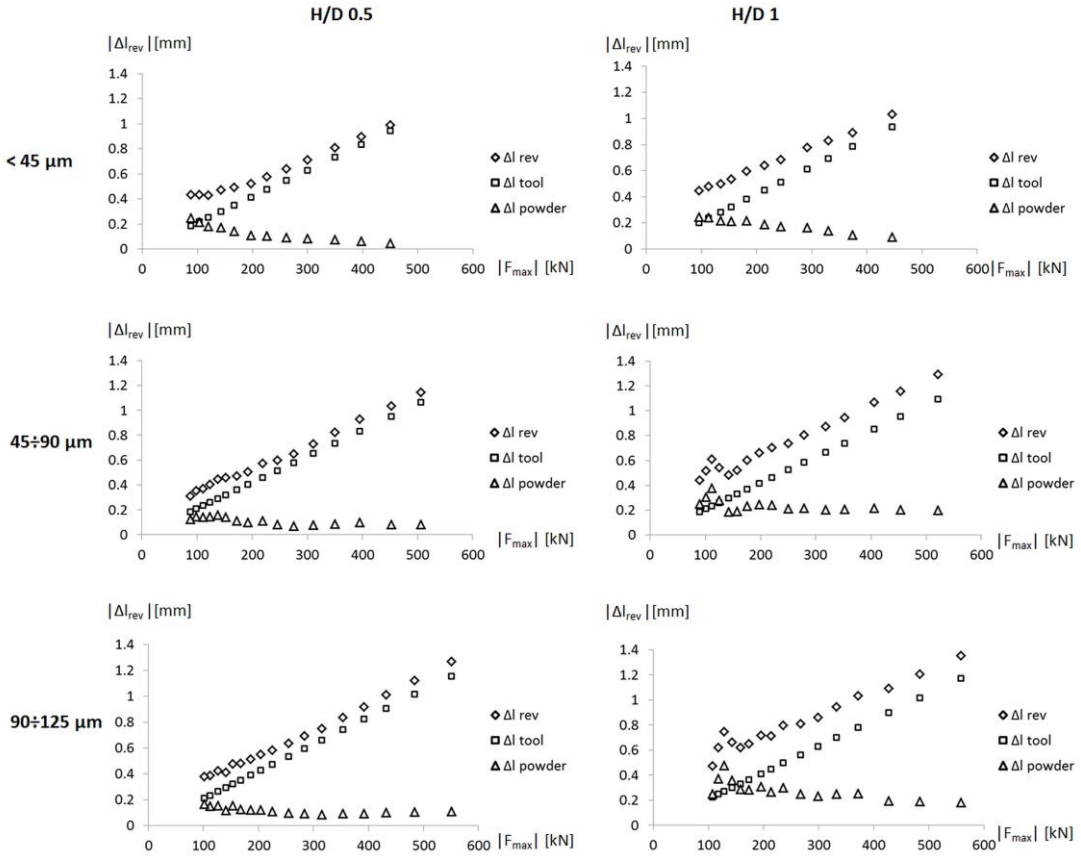

Figure 10. Reversible displacement vs. compaction force for each particle size and H/D ratio

The points relevant to the elastic displacement of the powder column (represented by triangles) are derived subtracting the contribution of the elastic displacement of the tools, which has been obtained experimentally using specimens, the stiffness of which is known.
In all the cases, slightly larger reversible displacements are observed at the highest H/D ratio, as a consequence of the larger permanent displacements, due to the plastic deformation, and the consequent strain-hardening (see figure 7), which will be discussed later on.
The influence of particle size will be now evaluated. In a solid material stiffness is supposed to be constant, so the elastic displacement increases with the applied force. In the specimens with the finest particle size, on the contrary, the elastic displacement tends to continuously

decrease on increasing the compaction force. This trend is related to the increase in the stiffness of the powder column due to the progressive densification and increased packing of powder particles on increasing the compaction force. In the specimens with higher particle size, however, the elastic displacement tends to slightly increase at the lower forces, up to approximately 150 kN, then decreases and tends to a stable value, according to the trend showed by the specimens with the finest particle size. This trend is especially evident at the highest H/D ratio, and might be related to the lower tap density, which determines more pronounced displacements due to the rearrangement in the first compaction step. Rearrangement increases density without an appreciable effect on stiffness, since densification is simply due to an increase in packing of the particles, without a significant growth of the interparticle contact areas. Above 150 kN, instead, the trend is determined by the progressive densification and corresponding increase in stiffness.

Permanent displacement is attributable to the powder rearrangement and to the plastic deformation of the powders as by equation (5)

$$\Delta l_{perm} = \Delta l_{rearr_{powder}} + \Delta l_{plast_{powder}} \tag{5}$$

Figure 11 shows the permanent displacement versus compaction force for each particle size and H/D ratio

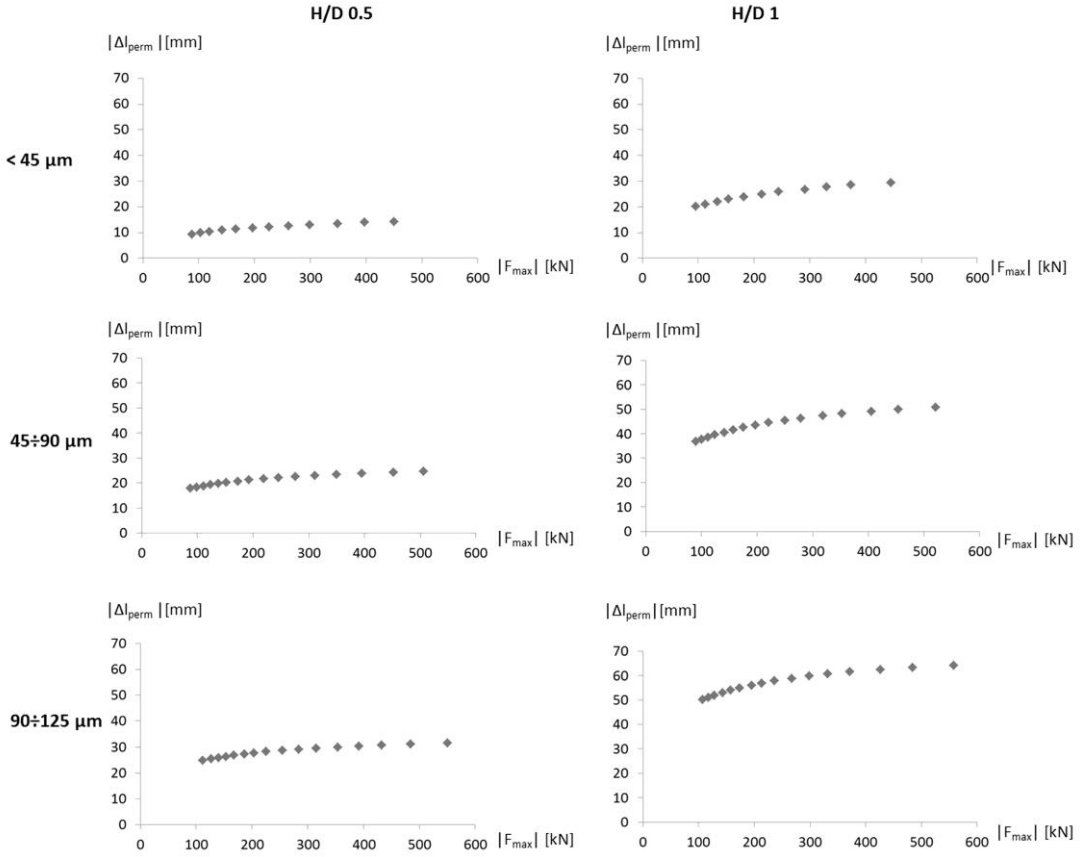

Figure 11. Permanent displacement vs. compaction force for each particle size and H/D ratio

Permanent displacement increases with particle size, due to the different tap density, which differently determines densification through rearrangement and plastic deformation. As expected, permanent displacement also increases with H/D ratio.

3.4 Reversible and permanent deformations

Aiming at obtaining from experimental data a model describing the behaviour of powder column during compaction, elastic and permanent deformations have been derived from the corresponding displacements, as by equations (6) and (7), where l_0 is the height of the powder column at zero displacement (X position measured when the punch contacts the powder and the die starts moving down - start of double action pressing)

$$\varepsilon_{el_{powder}} = \frac{\Delta l_{el_{powder}}}{l_0} \tag{6}$$

$$\varepsilon_{perm} = \frac{\Delta l_{rearr_{powder}}}{l_0} + \frac{\Delta l_{plast_{powder}}}{l_0} \tag{7}$$

The analysis is made referring to engineering strain and stress. The continuous densification determines an increase in the effective cross section, which might suggest to refer to true strain calculated as $\ln(l/l_0)$. Nevertheless, the continuous volume decrease of the powder column does not allow to calculate true stress as $\sigma(\varepsilon + 1)$, since this equation is derived assuming that the volume of the deformed body is kept constant. As mentioned in the introduction, the axial stress σ_a is the applied pressure and corresponds to the maximum stress applied to the powder column, obtained from the compaction force divided by the nominal contact area.

Figure 12 shows the elastic deformation of the powder column versus the stress applied, for each particle size and H/D ratio

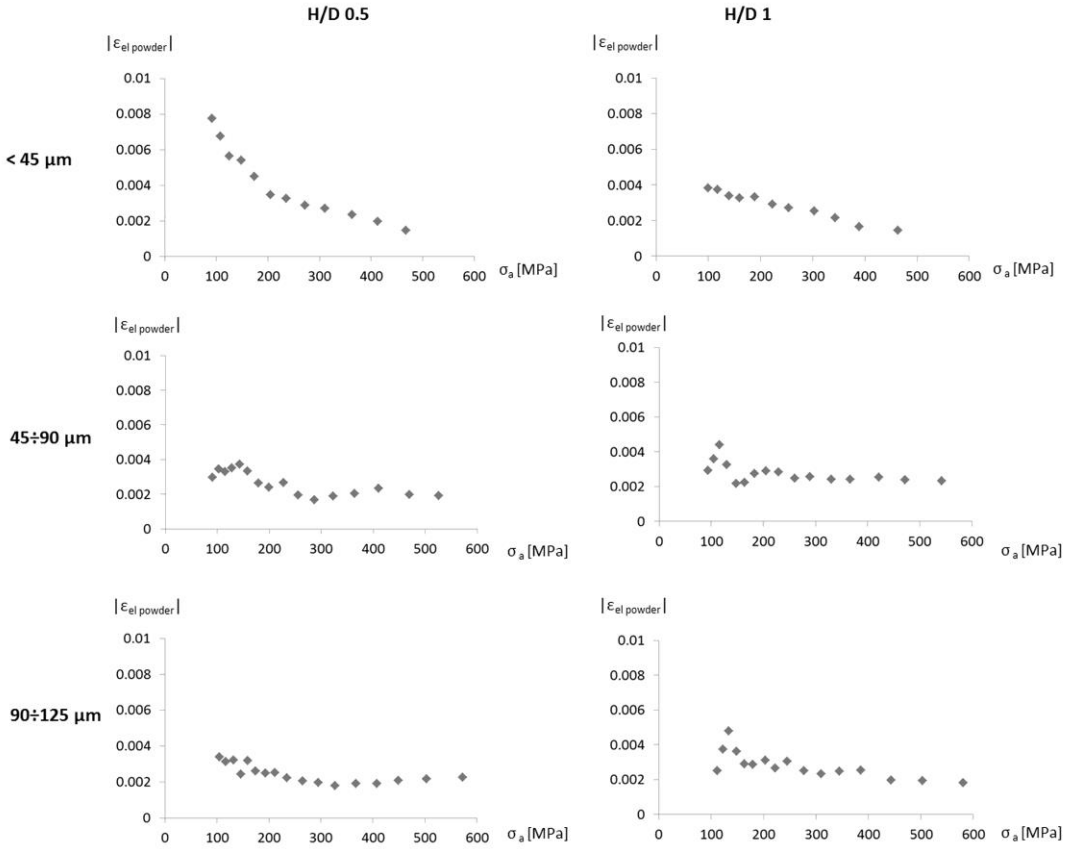

Figure 12. Elastic deformation vs. applied stress for each particle size and H/D ratio

The elastic deformation of the powder column during compaction confirms the trend displayed by the elastic displacement in figure 10. The ratio between the applied stress and the elastic deformation expresses the resistance to elastic deformation, and is given by *E* (elastic modulus) in uniaxial stress condition. During compaction, stress condition cannot be regarded as uniaxial, resulting from the compaction pressure and the radial constrain exerted by the die, and it varies during the whole process. Nevertheless, the ratio between the applied stress and the elastic deformation again expresses the resistance to elastic deformation, and it can be defined by an elastic constant K_{el}, as in equation 8

$$\sigma_a = K_{el}\varepsilon_{el} \tag{8}$$

Figure 13 shows the elastic constant K_{el} versus the applied stress for each particle size and H/D ratio.

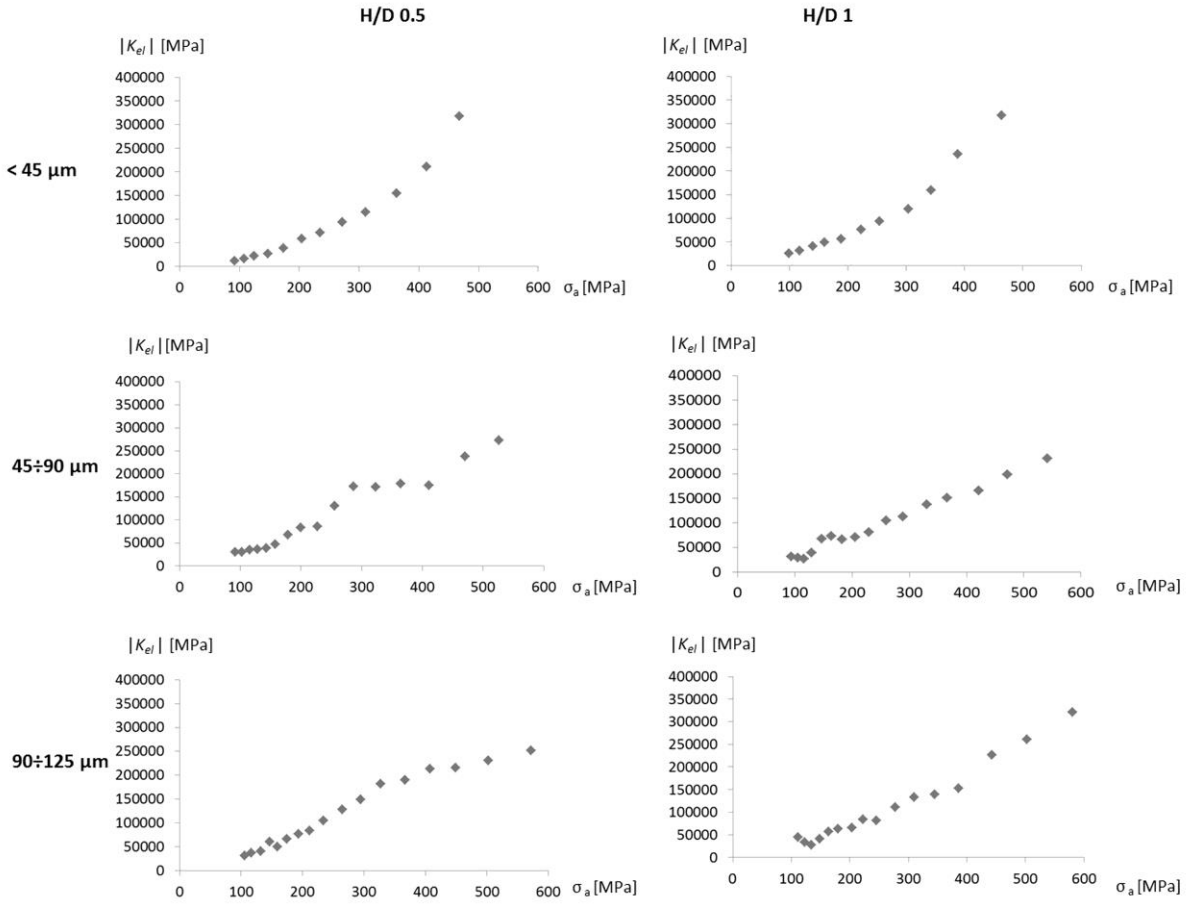

Figure 13. Elastic constant K_{el} vs. applied stress for each particle size and H/D ratio

K_{el} shows a trend, which is well related to the phenomena explained in paragraph 3.3. For the lowest particle size, in fact, due to the continuous densification K_{el} continuously increases, with an approximately exponential trend. For the higher particle sizes K_{el} is kept constant in the first compaction step, due to the contribution of rearrangement, and the resistance to elastic deformation tends to increase above the value, previously identified as the end of rearrangement (about 150 kN, corresponding to about 160 MPa). No significant influence of H/D ratio is observed in any case.

The permanent deformation, as defined in equation (5), versus the applied stress is shown in Figure 14 for each particle size and H/D ratio.

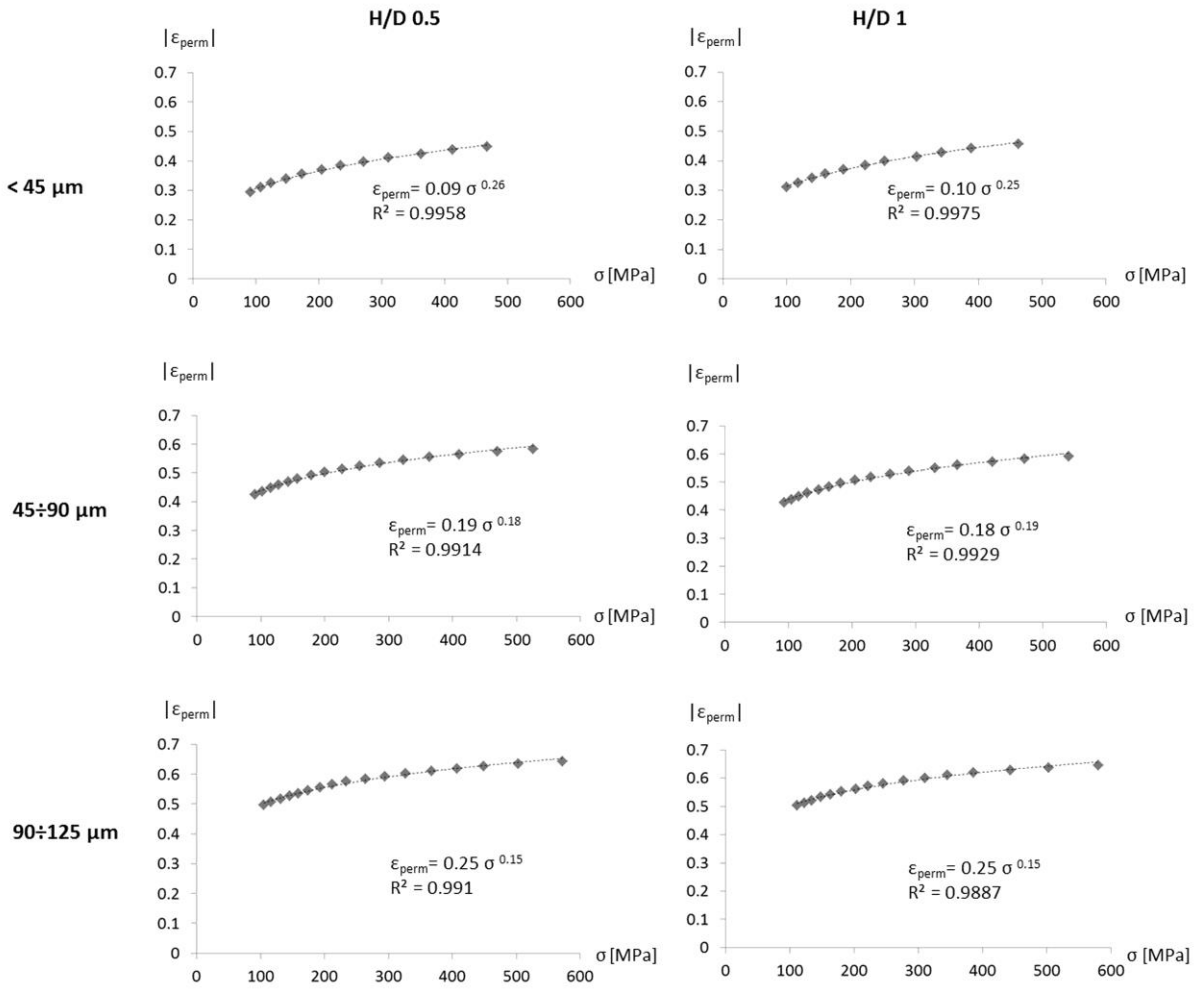

Figure 14. Permanent deformation vs. applied stress for each particle size and H/D ratio

The relationship between permanent deformation and applied stress is given by equation (9) that fits quite well the experimental data in the whole stress range investigated

$$\varepsilon_{perm} = K' \sigma^{n'} \tag{9}$$

Equation (9) does not formally represent the flow curve of the powder column, since it correlates the permanent deformation of the column, resulting from both rearrangement and plastic deformation, to the maximum applied stress. Nevertheless, equation (9) adequately describes the behaviour of the powder column, which determines densification. The parameter *K'* is directly related to the plasticity, and the parameter *n'* is inversely related to the resistance offered by the powder column to the increase in permanent deformation on increasing the axial stress. Both *K'* and *n'* depend on particle size, while the influence of H/D ratio is negligible, as shown in figure 15.

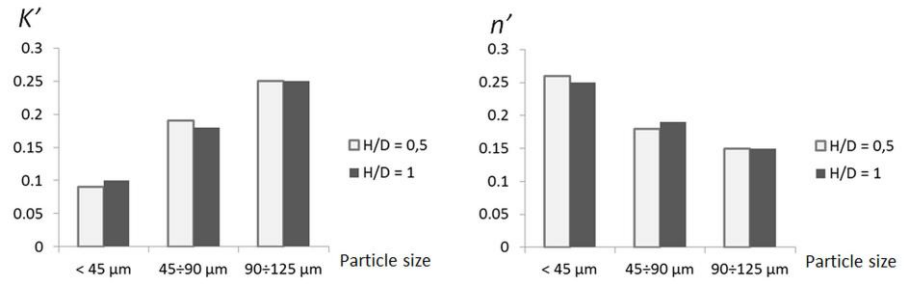

Figure 15. Influence of particle size and H/D ratio on parameters *K'* and *n'*

K' increases on increasing particle size, thanks to the higher permanent deformation due to rearrangement occurring in the specimens with the lower tap density: the lower the initial packing, the higher the effect of the increase in pressure on the rearrangement. Moreover, the lower internal frictional forces related to the lower extent of contact areas between larger particles may result in lower dissipation of force, and consequently again in a higher effect of the increase in pressure on the rearrangement. The larger contact areas developing between large particles imply a decrease in the effective pressure on the powder particles, and may also explain the decrease in parameter *n'* on increasing particle size, meaning a lower attitude to increase plastic deformation on increasing pressure.
Figure 15, showing the influence of particle size on *K'* and *n'*, highlights the same trend observed for *a'* and *b'*, the coefficients in the model describing the increase in density versus the applied pressure (see Figure 8), which is opposite to the trend observed for *a* and *b*, the coefficients in the model describing the density (see Figure 5). Densification is due to permanent deformation, so to model describing densification must be coherent with the model describing permanent deformation. The result above shows the need of considering tap density in describing densification: the model for the increase in density (equation (3)) has physical meaning, while the model for density (equation(2)) is purely a mathematical fitting.

The analysis of elastic deformation showed a different trend in the first compaction step, mainly due to the contribution of rearrangement, particularly evident in the specimens with the larger particle size. The contribution of rearrangement can be also highlighted in the curves displaying the permanent deformation, as shown in figure 16, where the different equations describing the deformation/stress relationship due to rearrangement and plastic deformation are distinguished.

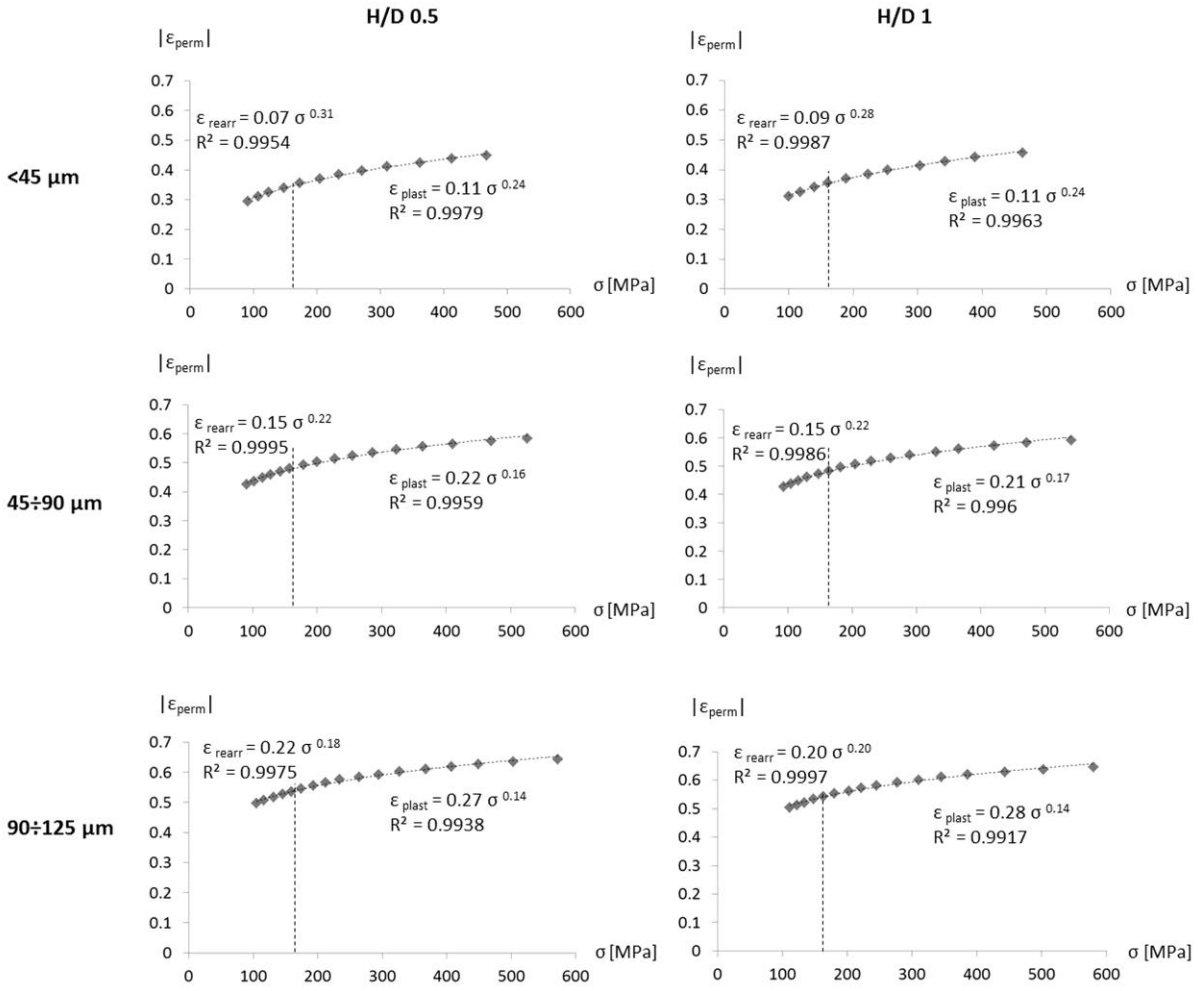

Figure 16. Distinguished contribution to permanent deformation vs. applied stress for particle size and H/D ratio

As expected, the higher slope of the curves in the part relevant to rearrangement is highlighted distinguishing the two contributions. As already observed, the curves tend to be less steep on increasing the stress (see figure 16), according to the higher resistance to plastic deformation, which is expected at higher stresses. The slope of the curves decreases on increasing particle size, both in the rearrangement and in the plastic deformation. No influence of H/D ratio is observed. Figure 17 compares *K'* and *n'* obtained for the curves representative of rearrangement and plastic deformation, along with the values obtained for the total curve; H/D 0.5 is reported, being the trend exactly the same for H/D 1.

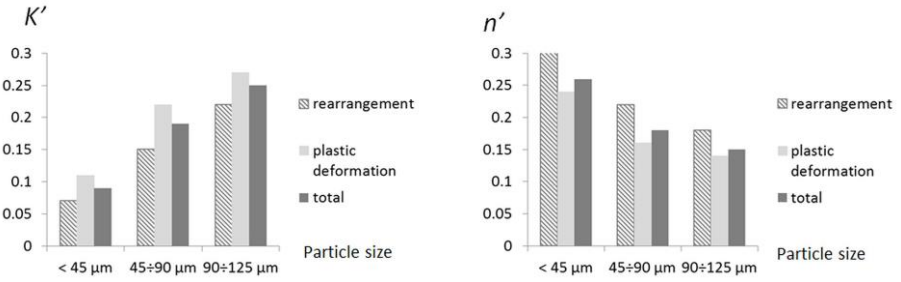

Figure 17. Influence of particle size on parameters *K'* and *n'* for the split curves - H/D 0.5

Parameters *K'* and *n'* describing the curve of permanent deformation versus the applied stress appear quite different if the contribution of rearrangement and plastic deformation are distinguished, or the whole curve is considered. To estimate the actual significance of these differences, figure 18 shows the permanent deformation vs. stress curves calculated considering a unique relationship between permanent deformation and applied stress in the whole range of applied stress (triangles), obtained considering the specific relationship determined in the rearrangement field (rhombus), and obtained considering the specific relationship determined in the plastic deformation field (squares).

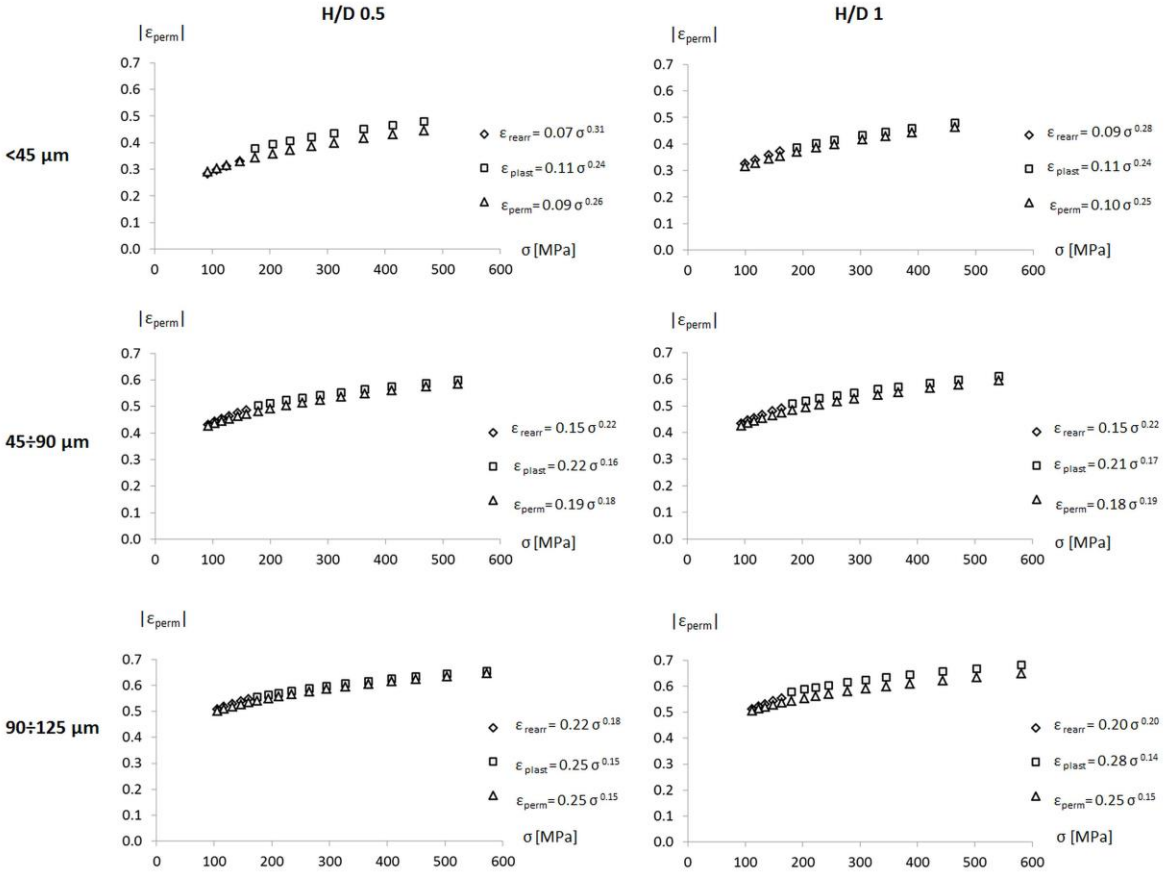

Figure 18. Permanent deformation vs. applied stress curves obtained considering different relationships for the different particle size and H/D ratio

The largest differences are observed in the curves showing the behaviour of the lowest particle size, lowest H/D ratio, and largest particle size, highest H/D ratio, mainly in the part relevant to plastic deformation. In the other cases curves are substantially overlapped. Nevertheless, it has been observed that the difference is mainly due to the number of digits considered for *K'* and *n'* in the curves fitting the experimental data. In fact, when three digits are kept, all the curves are overlapped, and the maximum difference observed among them is 2%, thus meaning that a unique relationship can be used to properly describe permanent deformation versus the applied stress.

4. CONCLUSIONS

The behaviour of AISI 316L powder column during uniaxial compaction was investigated in this work, considering different particle sizes (<45 µm, 45÷90 µm, 90÷125 µm). Cylindrical

specimens were produced in a rigid die, 35.01 mm diameter, at 6.5 g/cm^3 green density, and two different H/D ratios (0.5, 1). The data recorded by the press (force - displacement) have been used to experimentally derive an analytical model describing the behaviour of the powder during compaction, with reference to the column of powder within the die, and to the maximum axial stress on the powder column.
Main conclusions are following summarised.

- Densification curves for the different conditions have been derived and a model for densification is proposed, accounting for the influence of particle size.
- Both the force and the total displacement increase with the particle size, whilst no significant effect of the H/D ratio is observed. These results have to be related to the different tap density and to the dissipation of force due to friction.
- The trend of elastic and permanent displacement versus the compaction force highlights the different phenomena occurring during compaction, as affected by particle size.
- A reliable relationship describing the resistance to elastic deformation versus the stress applied, as affected by particle size, has been derived.
- A model describing the relationship between the permanent deformation and the stress applied for the different particle size and H/D ratios has been proposed, also distinguishing the contribution of rearrangement and plastic deformation.

An important result of this work deals with densification models: comparing the equations for densification and for permanent deformation, which have been obtained by independent data, it has been observed that only the model describing the increase in density is coherent with that of permanent deformation, thus meaning that it is the only one having a physical meaning.
These preliminary results show the influence of particle size and H/D ratio on the macroscopic behaviour of powder column during compaction, as derived from the data recorded by the press. Future work will also analyse the distribution of axial and radial stresses in the powder column, aiming at describing the behaviour of the powder.

References

[1] R.M. German, 'Green body homogeneity effects on sintered tolerances', *Powder Metallurgy*, 2004, **47**(2), 157-160

[2] A.C.F. Cocks, 'Constitutive modelling of powder compaction and sintering', *Progress in Materials Science*, 2001, **46**, 201-229

[3] P. Rossi, M.K. Alves, H.A. Al-Qureshi, 'A model for the simulation of powder compaction processes', *Journal of Materials Processing Technology*, 2007, **182**, 286–296

[4] L.N. Smith, P.S. Midha, A.D. Graham, 'Simulation of metal powder compaction, for the development of a knowledge based powder metallurgy process advisor', *Journal of Materials Processing Technology*, 1998, **79**, 94–100

[5] O. Coube, and H. Riedel, 'Numerical simulation of metal powder die compaction with special consideration of cracking', *Powder Metallurgy*, 2000, **43**(2), 123-131

[6] O. Coube, A.C.F. Cocks, C.Y. Wu, 'Experimental and numerical study of die filling, powder transfer and die compaction', *Powder Metallurgy*, 2005, **48**(1), 68-76

[7] W.M. Long, 'Radial pressures in powder compaction', *Powder Metallurgy*, 1960, **6**, 73-86

[8] B. Wikmann, N. Solimannezhad, R. Larsson, M. Olderburg, H.A. Haggblad, 'Wall friction coefficient estimation through modelling of powder die pressing experiment', *Powder Metallurgy*, 2000, **43**(2), 132-138

[9] E. Ernst, and D. Barnekow, 'Pressure, friction and density during axial powder compaction', Proceedings 'PM '94 Powder Metallurgy World Congress', 1994, Paris, France, 6-9 June 1994, EPMA, Shrewsbury (UK), 673-676
[10] H.A. Al-Qureshi, A. Galiotto, A.N. Klein, 'On the mechanics of cold die compaction for powder metallurgy', *Journal of Materials Processing Technology,* 2005, **166**, 135–143
[11] H.A. Al-Qureshi, M.R.F. Soares, D. Hotza, M.C. Alves, A.N. Klein, 'Analyses of the fundamental parameters of cold die compaction of powder metallurgy', *Journal of Materials Processing Technology,* 2008, **199**, 417-424
[12] G.F. Bocchini, Friction on punch faces and its effect on the Green density of PM parts', Proceedings 'PM '94 Powder Metallurgy World Congress', 1994, Paris, France, 6-9 June 1994, EPMA, Shrewsbury (UK), 741-744
[13] D. Poquillon, J. Lemaitre, V. Baco-Carles, Ph. Tailhades, J. Lacaze, 'Cold compaction of iron powders-relation between powder morphology and mechanical properties. Part I: Powder preparation and compaction', *Powder Technology,* 2002, **126**, 65-74
[14] E. Olsson, and P-L Larsson, 'On the Effect of Particle Size Distribution in Cold Powder Compaction', *Journal of Applied Mechanics,* 2012, **79**, 051017, 1-8
[15] R.M. German, J. Ma, X. Wang, E. Olevsky, 'Processing model for tungsten powders and extension to nanoscale range', *Powder Metallurgy,* 2006, **49**(1), 19-27
[16] E. Olevsky, and A. Maximenko, Nonstationary problems of the quasistatic theory of hardening plastic bodies', *Computational Materials Science,* 1994, **3**(2), 247-253
[17] G. Rong-de, 'A New Powder Compaction Equation', *The International Journal of Powder Metallurgy,*1991, **27**(3), 211-216
[18] J. Secondi, 'Modelling powder compaction – From a pressure-density law to continuum mechanics', *Powder Metallurgy,* 2002, **45**(3), 213-217
[19] G. Aryanpour, M. Farzaneh, 'Application of a piston equation to describe die compaction of powders', *Powder Technology,* 2015, **277**, 120-125
[20] I. Cristofolini, M. Pilla, D. Belluzzi, M. Crocetti, A. Molinari, 'Experimental Study of Sizing of Gears by a Hydraulic Press Proceedings EURO PM2012 Congress & Exhibition, Basel 16-19 September 2012', ed. EPMA, Shrewsbury (UK), **1**, 501-506
[21] I. Cristofolini, M. Pilla, D. Belluzzi, G. Pederzini, M. Crocetti, A. Molinari, 'Influence of the Scatter of Sintered Height on the Precision of Parts Sized by a Hydraulic Press', CD Proc. 'Euro PM2013 Congress & Exhibition', Gotheborg, Sweden, 15-18 September 2013
[22] I. Cristofolini, V. Fontanari, D. Belluzzi, G. Pederzini, A. Molinari, 'Experimental study of the relationships between sizing force and deformation of sintered parts to define a process control procedure', *Powder Metallurgy,* 2014, **57**(5), 394-400
[23] I. Cristofolini, A. Molinari, D. Belluzzi, G. Pederzini, M. Federici, In Situ Analysis of the Powder Behaviour during Cold Compaction, CD Proc. 'Euro PM2014 Congress & Exhibition', Salzburg, Austria, 21-24 September 2014
[24] I. Cristofolini, A. Molinari, G. Pederzini, M. Piva, A. Grandi, 'From Experimental Data an Analytical Model of Powder Behavior During Uniaxial Cold Compaction', proceedings 'PowderMet 2015', San Diego – CA, 17-20 May 2015, **1**, 19-30

List of Figure Captions